Mimics Image Reconstruction for Computer-Assisted Brain Analysis

Andreas A. Linninger, Michalis Xenos, Srinivasa. Kondapalli, MahadevaBharath.R. Somayaji
Laboratory for Product and Process Design, Departments of Chemical and Bio- Engineering,
University of Illinois at Chicago, Chicago, IL, 60607, USA.
Email: linninge@uic.edu

David C. Zhu* and Richard Penn**
Departments of Radiology* and Neurosurgery**, University of Chicago.

Abstract

Societal Relevance. Diseases of the central nervous system such as Alzheimer, Parkinson and Huntington are affecting millions of people around the world. Despite progress in science and medicine, the treatment of brain diseases is hampered by the complex inner organization of the central nervous system (CNS). Novel analytical imaging techniques like MRI, functional MRI, Diffusion Tensor Imaging (DTI), CT, Positron Emission Tomography (PET), etc, improve medical diagnosis; however, quantitative use of the imaging data for devising better treatment options for a specific patient are not possible with existing technology. The current lack of basic understanding of the intracranial dynamics also prevents the implementation of effective invasive drug delivery into the brain. In addition, without models for quantifying the intracranial pressure and flow of cerebrospinal fluid, more effective treatment of patients suffering from hydrocephalus cannot be expected. There is a need for better qualitative analysis of imaging data of the human brain.

Innovation. This paper proposes a novel computer-assisted brain research approach by integrating Mimics image reconstruction capabilities with first principles models for transport phenomena in the human brain. We present the information flow for embedding cutting-edge brain MR imaging data into advanced computational tools for achieving a better quantitative understanding of complex intracranial dynamics. This novel software- hardware integration will provide for the first time detailed information for abnormal ventricular sizes and accurately predict blood and cerebrospinal fluid (CSF) flow inside the brain. Other innovations include predictions of the penetration depths of drugs into specific regions of the brain. The therapeutic potential for these novel approaches will be supported by means of two specific examples. The first one focuses on new insights pertaining to the changes in intracranial pressures (ICP) and CSF flow dynamics in hydrocephalic patients. The second example will highlight new avenues for the systematic design of invasive drug delivery techniques based on patient-specific image data and molecular transport properties of neuro-pharamacological drugs.

Potential. These results demonstrate the proof-of-concept for a novel computer-assistant brain research approach. At the heart of this novel technique, Mimics image conversion provides a critical bridge between patient-specific data and advanced computational transport models. The unique integration of imaging data and computational analysis using advanced volume and finite element methods helps to reconstructs accurately flow and pressure fields inside the brain, quantifies fluid structure interaction between the vascular bed and the neurons (gray and white matter of the brain parenchyma) and predicts achievable drug delivery pathways inside the complex brain geometry. The link between images and computational analysis facilitated by Mimics is expected to advance the effectiveness of scientists and engineering in assisting medical diagnosis and treatment planning. The successful implementation of these novel techniques might make Mimics a central element of the medical diagnostic infrastructure of hospitals treating brain diseases. The computer-assisted brain analysis may become a standard extension of the existing patient care.

1. Introduction

Relevance. During the last decades, progress in clinical analysis and diagnosis is very rapid and several new imaging techniques have been developed or gained significant advances in accuracy (MRI, fMRI, CT, PET etc). However, these advanced techniques do not fully benefit the prospects of patients since physicians often use the data merely in a qualitative sense. It is also hard for MR analysis to translate detailed patient data into a consistent picture of abnormal brain conditions without the link to computational analysis methods. For example, it is possible to accurately measure the CSF flow with phase cine MRI in vivo, the corresponding intracranial pressure (ICP) which is critical to assess the patients' status is only accessible by using fluid mechanic calculations. MR imaging is also not directly able to incorporate deformation effects of the solid brain matrix due to the limited resolution of the images (~1mm).

Complexity. A second knowledge barrier exists due to complexity of the human brain. It is an organ composed of porous tissues (gray and white matter) embedded in CSF. The cell matrix of the brain called parenchyma consists of two compartments. The gray matter is composed mainly of the neurons (soma) and glial cells, while the white matter provides neural connectivity by means of the axons. The parenchyma is embedded in cerebrospinal fluid creating buoyancy and providing a hydrodynamics shock protection for the sensitive neurons. The CSF is produced in the choroid plexus and flows into central fluid filled cavities called the ventricular space. CSF is produced in a pulsating manner at the choroids plexus in the center of the brain. The ventricles are connected through foramina giving rise to a linked network composed of two lateral, a third and a fourth ventricles which lead to the spinal and cranial subarachnoid spaces (SAS) through the foramina of Magendie and Luschke (Figure 1), (Kandel et al, 1991, Egnor et al, 2002, Ammourah et al, 2003). Even though abnormal CSF flow dynamics are responsible for a

Figure 1. Brain Physiology

number of brain disorders (Hakim et al, 1976, Nagashima et al, 1990), the pathological patterns of intracranial dynamics in diseases like Hydrocephalus are still poorly understood.
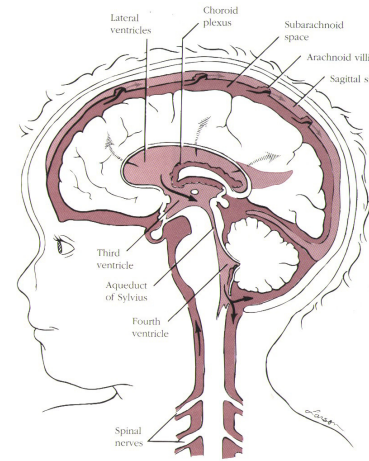
The brain parenchyma also possesses a complex microstructure as seen in Figure 2. Note that in the center of the organ there is a concentration of gray matter, the Striatum and is composed of two substructures, the Caudate striatum and the Putamen (Kandel et al, 1991). It is known that certain pharmacological drugs provide relief against diseases of the central nervous system (CNS) if the drug can be delivery into the relevant areas such as the Putamen. Hence, the certain areas of the brain stem are targets of invasive drug delivery applications. Despite this knowledge, it is not obvious how to deliver the drug without hurting any important brain tissue and at the same time permeating the area of interest in high enough dosis to ensure therapeutic drug efficacy. It would be desirable to have tools that allow the physician to use the patient-specific images in combination with computer-assisted transport models to accurately specify the position for the injection (Drug delivery into Human Brain). Moreover, guidance for surgical procedure based on patient-specific images and computational models of the individual's CSF flow characteristics would create more effective treatment options for patients suffering from hydrocephalus (Specific shunt characteristics for each individual).
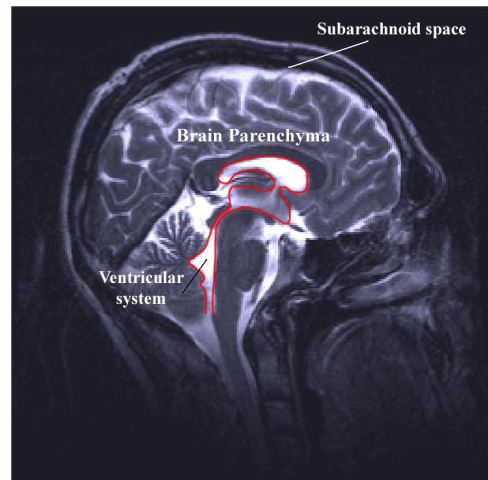

Figure 2. MR image of a healthy human brain

Outline. This paper proposes a novel computer-assisted brain analysis approach by integrating Mimics image reconstruction capabilities with first principles models for transport phenomena in the human brain. Section 2 gives an overview of the proposed computer assisted methodology. It will aim at enhancing the value of clinical images for diagnostic and therapeutic options by creating a seamless information flow integrating patient-specific data with computational

methods for transport processes in the brain. Two particular applications will be shown in more detail. The first presented in section three will show how the reconstruction techniques with Mimics for deducing brain geometry and CSF flow in the venticules. The second example in section four discusses the role of image reconstruction in the service of systematic drug delivery techniques. The paper closes with conclusions.

2. Computer-assisted brain analysis - Methodology

Recent advances in clinical diagnosis provide a wealth of ever more accurate data to the clinician. MR imaging by advanced scanners such as the 3T GE Signa system (GE Medical Systems, Milwaukee, WI) at the University of Chicago produce high precision images of the brain and its microstructure. Analysis of the T1 images permits the determination of the water content in the gray and white matter (Penn et al, 2005). Recently, we demonstrated that CINE phase contrast technique can even measure the CSF flow in vivo (Linninger et al, 2005). Even the small expansions of the ventricles during each cardiac cycle collaborator Zhu was able to measure with high accuracy (Zhu et al, 2005). Finally, Diffusion Tensor Imaging (DTI) provides exact orientation of the diffusivity and local differentiation of the neural pathways in the white matter of the human brain. However, this rich information is used currently only qualitatively for diagnosis. A detailed computational analysis of the clinical data would provide a significant advancement that is currently only in its infancy.

Therefore, we have developed a *computer-assisted brain analysis* methodology presented in Figure 3. On the left, the current state-of-the-art with mere image observation is displayed. We collect MR data using a powerful 3T GE Signa scanner (GE Medical Systems, Milwaukee, WI)) located at the Brain Research imageing Center (BRIC) at the University of Chicago. Mimics (Materialise Inc, 2004) provides a critical link for converting the embedded data into mathematically precise geometric information. The output from the MR images reconstruction with Mimics is a precise three-dimensional patient specific geometry of the brain or a subsection of it. This step is known as *image reconstruction*.

The discretized brain geometry information composed of volumes and boundary surfaces is passed into commercial grid generator tools (e.g. Gambit (The Fluent Inc, 2005), GID (CIMNE – GID, 2005)). The *grid generation* step segregates the geometry data exported from Mimics into a computational mesh with well-defined mathematical properties and specific file format. This step is also known as triangularization (Bohm et al, 2000). The computational grid composed of a fine mesh of tetrahedrons or polygons serves as input to the detailed computational analysis of transport phenomena in the brain. This computational step involves scientific computation algorithms for the numerical solution of conservation balances for mass, species transport, momentum and energy. The solution of these partial differential equations (PDE) with commercial tools like Fluent (The Fluent Inc, 2005), StarCD (CD-Adapco, 2005), Ansys (ANSYS Inc, 2005), allow for the computation of properties of interest such as the flow rate, velocities and pressures of blood in the cerebral system (Kondapalli and Linninger, 2005) or cerebrospinal fluid in the ventricular system. In other instances, stresses and strains of the brain parenchyma or its shift in water content are the subject of these transport equations. We will refer to these basic conservation laws of mass, momentum and energy as first principles, because no abstract modeling assumptions (e.g. electric circuit analogies, spring dashboard analogy) are used. This approach also needs only a small number of physical constants such as CSF viscosity and density. In parallel to existing commercial tools, our group has developed a suite of hybrid simulation algorithms for large-scale sparse differential algebraic systems (Chowdry and Linninger, 2001, Bahl and Linninger, 2001), finite volume and finite element proprietary code (Xenos, and Linninger, 2005b) in order to extend the capabilities of the computational analysis beyond the limitations of commercial tools. In particular, our research is active in fluid structure interaction of porous brain tissue, water shift caused by elevated intracranial pressures (ICP).

Finally, post-processing steps involve graphical image rendering, visualization and animation of computational results. The entire information flow proposed in Figure 3 was highly automated by creating flexible interfaces between different tools with the goals of minimizing the user intervention in computer-assisted brain analysis.

In the next section, we will demonstrate actual results of ongoing research in which the novel computer-assistant approach was used to address open questions in brain disorders like Hydrocephalus, Neurological disorders and brain tumors.
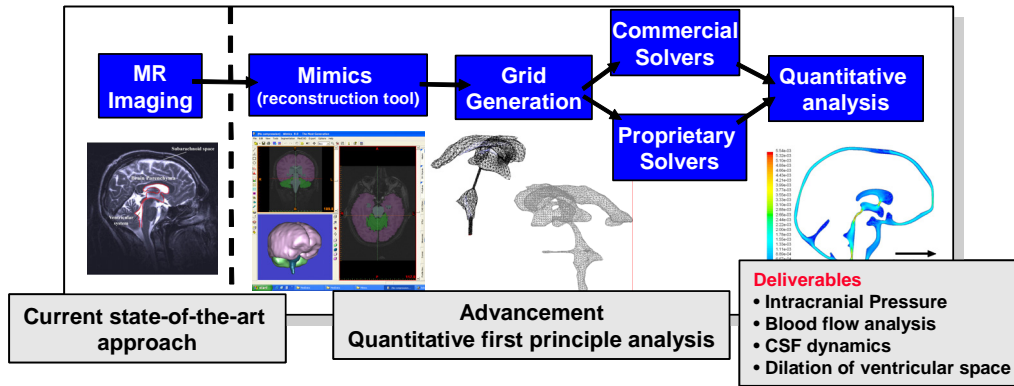
Figure 3. Schematic of the workflow in the computer assisted diagnosis approach

3. Three-dimensional patient specific CSF flow dynamics

The first problem concerns uncertainty pertaining to the intracranial dynamics leading to the enlargement of the ventricular system. The condition of enlarged ventricles known as hydrocephalus affects 70,000 people each year causes headache, gait problems and if untreated may be fatal. Despite detailed studies of the pattern and timing of CSF motion with MRI techniques (Enzmann and Pelc, 1992) the causes and mechanical principles underlying intracranial dynamics of hydrocephalus are still controversial. Early authors conjectured that large ICP differences between the ventricles and the subarachnoidal space are responsible for hydrocephalus to develop. Our recent studies with mongrel dogs show that communicating hydrocephalus is inconsistent with large tranmural pressure differences (Penn et al, 2005). This result was validated with the computer-assisted-brain research approach (Xenos and Linninger, 2004, Linninger et al, 2004) whose main milestones will be presented next.

3.1. Exact reconstruction of the CSF pathways

The brain is embedded in fluid called the CSF. CSF is generated in four central cavities at the base of the brain called the ventricles. The ventricles are connected through the foramina and lead to the outer side to the brain into a large reservoir called the spinal and cranial subarachnoid spaces (SAS) through the foramina of Magendie and Luschke. In the first state of this approach, the detailed three-dimensional geometry of the CSF filled ventricles had to be extracted for an actual patient. We acquired MR data of the brain geometry of a 32-year-old healthy volunteer at the BRIC. The complex pathways of the ventricles (show in yellow in Figure 4) and the cerebral subarachnoidal space (shown in red in Figure 4) were reconstructed with the help of Mimics (Materialise Inc, 2004). For this volunteer, the ventricles were found to contain 9.8cc of CSF, the cerebral SAS measured 36ml. For the accurate reconstruction of the ventrcilar cavities and the subarachnoidal space, 120 MRI slices of a healthy human subject were imported into Mimics. The specific structures of interest were "*colored*" with the help of the layer tool on each slice. This approach allows us to separate the CSF filled spaces from the rest of the brain. The resulting information was exported as three-dimensional models and polylines. Once the three-dimensional objects have been created, they can be exported for use with other utilities as '.*stl*' (STL) files using the *STL+* Module. Contours of the specific brain sections were extracted from the sagittal slices by selecting the desired '*layer*' and choosing the '*Calc Poly*' option.

Figure 4. Three-dimensional reconstruction of the CSF pathways: ventricular system (yellow), cerebral subarachnoidal space (red).

3.2. Triangularization of three-dimensional CSF filled spaces

The next step aimed at converting the Mimics geometry into a computational grid. Therefore, the extracted geometric information was introduced into suitable grid generators (e.g Gambit by The Fluent Inc, 2005). Gambit has the advantage of full integration with the popular computational fluid dynamics tool Fluent. The file exchange benefits from standardization of the face and volume data via *STL* or *IGES* file formats. A direct triangularization with Mimics features without third party grid generators should be possible by virtue of direct file exchange of
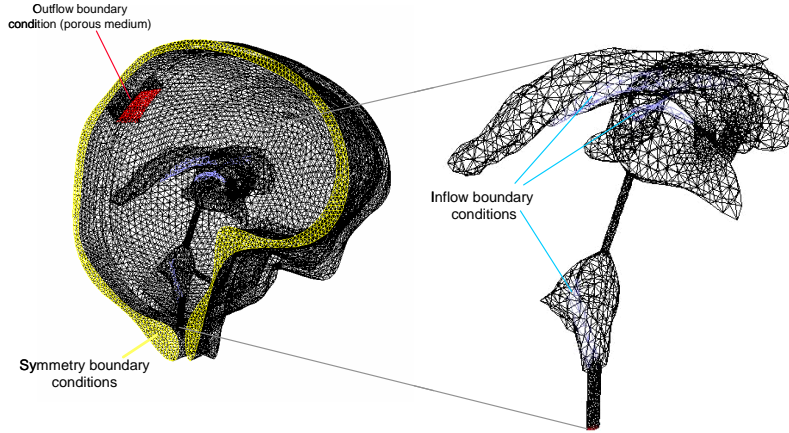

Fluent mesh formats (**.msh*). In order to prepare the raw volume and surface data for further computational analysis, grid generation involves the specification of well-defined boundaries. In Figure 5, the yellow surface constitutes a symmetry line of the brain's left hemisphere. The re-absorption in the subarachnoidal villi is rendered as an area of porous mass transfer between the CSF in the subarachnoidal space and the venous sagittal sinus depicted in red. Figure 5 (right) also depicts the detailed mesh for the four cerebral ventricles connected by the narrow aqueduct of Sylvius linked to the subarachnoidal

Figure 5. Definition of boundaries and meshed geometry of the ventricular system and cerebral subarachnoidal space.

space by the foramen of Monro. The meshed geometry with the boundary conditions of Figure 5 led to a computational grid composed of 59405 tetrahedral elements and 16771 nodes.

3.3. Computational fluid dynamics model of intracranial dynamics

Given the exact dimensions of the ventricular system, it is now possible to apply first principles to compute accurately the CSF flow and pressure field in the brain. Its movement is driven by the CSF production in the choroid plexus and the pulsating motion of the parenchyma in response to the expansion of the vascular bed during each peak of the cardiac cycle (Linninger et al, 2005). The first principle approach leads to fundamental balance equations for conservation of mass and momentum without resorting to naïve analogies (e.g electric resistor analogy, spring dashboard analogy). These balances applied to the complex three-dimensional brain geometry lead to partial differential equations known as the continuity and the Navier-Stokes equations (Schlichting, 1979). The governing equations for the Newtonian CSF flow in the ventricular system are given in equations (1) and (2).

$$\vec{\nabla} \cdot \vec{q} = 0 \tag{1}$$

$$\frac{\partial \vec{q}}{\partial t} + (\vec{q}.\vec{\nabla}\vec{q}) = -\frac{1}{\rho}\vec{\nabla}p + \nu\,\vec{\nabla}^2\vec{q} \tag{2}$$

where $\vec{q}$ is the velocity vector and ρ is the density of CSF and ν is the kinematic viscosity ($\nu = \mu/\rho$). For this study, porous boundary conditions were used to account for CSF reabsorption through arachnoid villi (Bear and Bachmat, 1990, Dullien, 1979).

The discretization method of the N-S equations used in this paper is the Finite Volume method. Fluent is using this approach with the SIMPLE algorithm (Patankar, 1980) based on a staggering grid approach as unlike conventional methods (see MAC method (Fletcher, 1991)). From the other hand our in build codes are using more advanced approaches facilitation the Finite Volume approach with the use of inexact Newton for the nonlinear system and a Krylov space based method for the linear subsystem. In our solvers we have refined high-speed sparce matrix solution techniques based on Krylov subspace iterations (GMRES, Arnoldi algorithm) (Chowdry and Linninger, 2001, Bahl and Linninger, 2001). Finally both solvers use he Generilizes Curvilinear Coordinates in order to describe complex geometries as the brain complex structure (Xenos, and Linninger, 2005a).

3.4. Results - Pulsatile CSF flow in the normal human brain

The solution of the large-scale transport problems for a normal subject rendered the complete three-dimensional CSF flow and pressure fields as a function of time (Linninger et al, 2005). To the best of our knowledge, the intracranial dynamics in 4D have not been reported before in the open literature. Figure 6a-d displays thirty vertical plane projections of the three-dimension velocity field at four different time steps during the cardiac cycle. The pulsating motion of the CSF peaks at the systole (i.e. 0.44sec). Highest velocities were observed in the foramina. In all ventricles, CSF recirculation was observed. The highest velocity occurs in aqueduct of Sylvius, 9.2×10^{-3}m/sec (peak of the pulsation-0.44sec). This value is in good agreement with clinical measurements of the CSF flow for the same individual using advanced Cine phase contrast imaging techniques (Linninger et al, 2005). The velocity vectors do not significantly change in the SAS with maximum of 2.4×10^{-4}m/sec. CSF pulsations are observed near the foramina of Magendie, the arachnoid villi and sagittal sinus. In most of the subarachnoidal space, velocity pulsations dissipate very quickly. Figure 7 shows two snapshots of the hydrostatic pressure (ICP) of the CSF. In these dynamic simulations, we found the ICP of 500 Pa above the venous pressure. This value is consistent with physiological conditions measured independently (Penn et al, 2005).
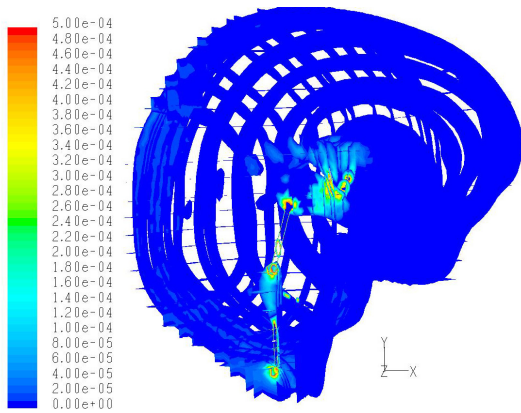

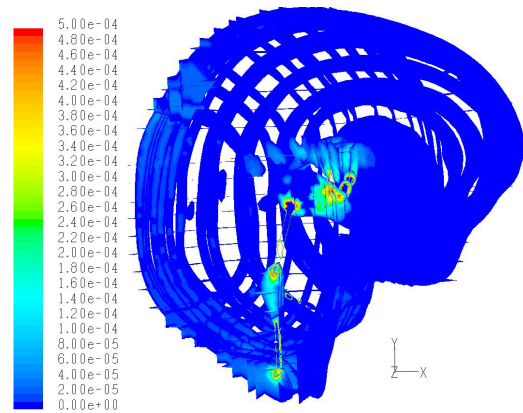Figure 6a. Detailed CSF flow field for t = 1.0s

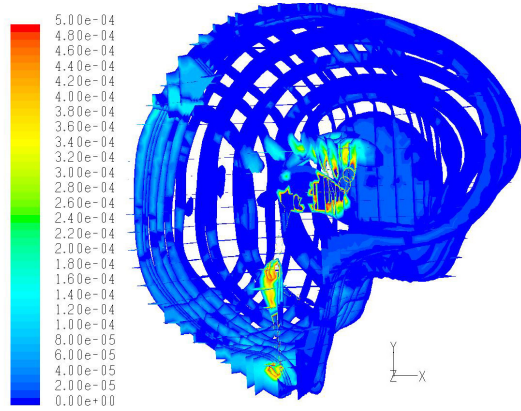Figure 6b. Detailed CSF flow field for t = 1.2s
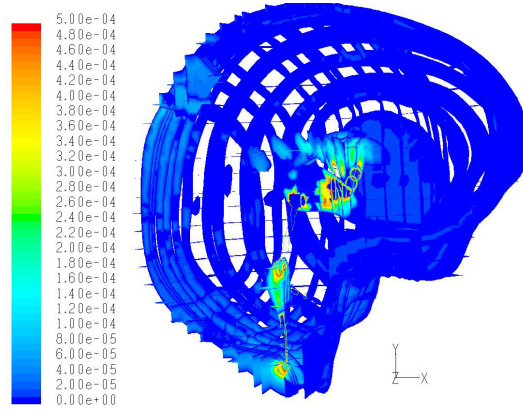

Figure 6c. Detailed CSF flow field for t = 1.5s
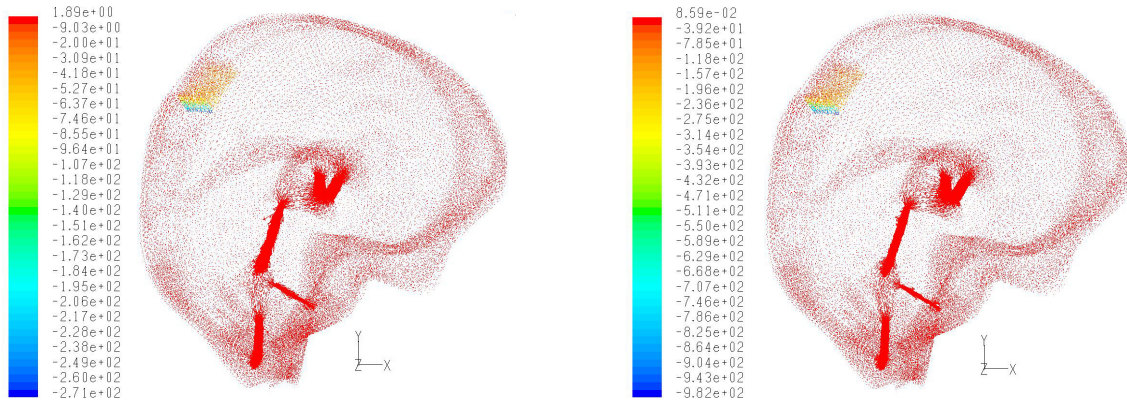

Figure 6d. Detailed CSF flow field for t = 1.8s

Figure 7. Static pressure fields for t = 1.2 and 1.5 s

3.5. Results for the Hydrocephalic Brain

A breakdown in the CSF reabsorption mechanism leads to a pathological condition of drastic volume increase of the ventricle. The conditions known as hydrocephalus is depicted Figure 8. The total ventricular volume may reach 180cc, which is more than 10 times the normal value. At the same time, the intracranial pressure (ICP) increases dramatically up to 5000-6000 Pa. Such elevated pressures may cause a breakdown of the blood supply to the brain – a life threatening condition. Figure 9 demonstrated simulated results produced with our computer-assisted brain analysis approach for a hydrocephalic brain. In hydrocephalus, the compression of the brain cell matrix due to the CSF accumulation must be considered. This is a complex fluid-structure interaction problem in which the equations of motion for the solid, cf eqs (3)-(4) are fully linked with fluid flow equations of a porous medium (Biot, 1941).

$$G\vec{\nabla}^2\vec{q} + \frac{G}{1-2v}\vec{\nabla}\varepsilon - \alpha\vec{\nabla}P = 0 \qquad (3)$$

$$k\nabla^2 P = \alpha\frac{\partial\varepsilon}{\partial t} \qquad (4)$$

Equation (3) describes the displacement of the solid matrix and equation (4) describes the fluid pressure throughout the porous brain parenchyma. G is a constant called complex shear modulus $(G = E/2(1+v))$, E is the Young's modulus and v is the Poisson's ratio. Where α is a term that measures the ratio of the water volume squeezed out to the volume change of the medium and k represents the permeability of the porous medium.
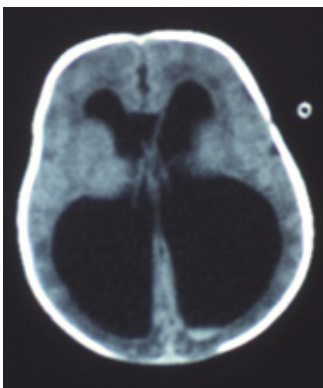

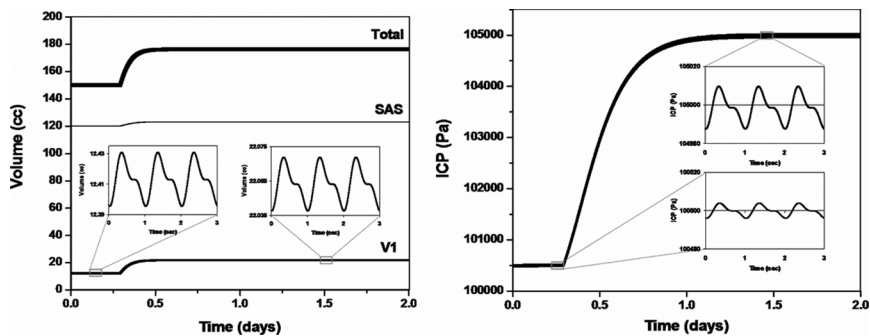Figure 8. A horizontal cut of a hydrocephalic brain with enlarged ventricles

Figure 9. Ventricular enlargement (left) and ICP increase (right) during the formation of acute hydrocephalus.

7

4.   Three-dimensional patient specific drug-delivery into the human brain

Invasive techniques provide a direct approach to administering drugs across the blood brain barrier (BBB). The efficacy of invasive techniques is measured in terms of the penetration depth enabling the drug to penetrate directly into the site of interest. Unfortunately, many experimental studies on drug delivery report insufficient penetration depths when relying of diffusion only (Morrison et al., 1994, Bobo et al., 1991, Hamilton et al., 2001). Novel approaches to enhance drug perfusion by imposing a convective bulk flow field in the extracellular space are promising. However, there is no adequate data for designing convection-enhanced drug infusion policies in human subjects.

Morrison et al., 1994 presented the advantages of high flow micro-infusion for delivering macromolecules to the brain with the help of a one-dimensional model. Kalyanasundaram et al. (1997) and Reisfeld et al., (1995) discussed the two dimensional transport of chemical species by including both the diffusive and convective contributions using Finite Element Method (FEM). None of the previous approaches takes into consideration the three-dimensional brain physiology and the strong directionality of the axons in the white matter. These effects associated with the anisotropic and inhomogeneous properties of the brain tissue influence the achievable penetration depths and must be considered for the design of drug delivery options to be realistic. Moreover, none of the previous studies includes catheter design considerations, which are essential for implementing any drug delivery therapy. The subsequent section introduces a completely novel approach for drug delivery into the human brain based on three-dimensional first principles transport phenomena.

4.1. Three-dimensional reconstruction of the specific human brain parenchyma

The major challenges in the drug delivery problem are as follows:
- accurate geometric reconstruction of the brain physiology, e.g. gray matter, white matter, specific targets of brain subregions in the brain stem
- quantification of the anisotropic inhomogeneous properties of the brain tissue, e.g. diffusivity, tortuosity, permeability and porosity
- accurate prediction of the infusate flow field (drug dilated in water) within the intracellular space.

We extracted the detailed composition of the three-dimensional brain parenchyma from MR images with Mimics. The cell matrix can be separated into several compartments with different transport properties (diffusivity, tortuosity, permeability and porosity). Figure 10 clearly delineates the Cerebral Cortex (pink), brain stem (blue) and the Cerebellum (green). The parenchyma (pink) is further divided into gray and white matter; the brain stem consists of the mesencephalon, pons, putamen, and medulla oblongata. The detailed physiologically consistent 3D geometry the patients' brain was transformed into a computational grid with the methods described in Figure 3. Figure 11 shows a vertically positioned catheter inserted into the gray matter of the left hemisphere. Results of this very realistic setting will be discussed in the next subsection.
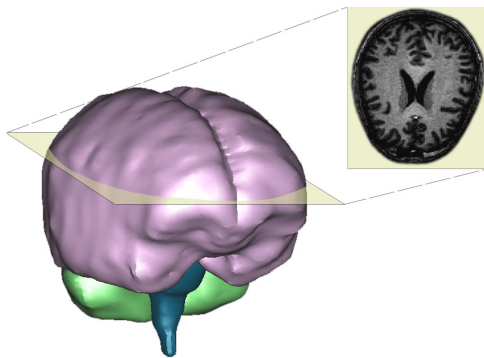

Figure 10. Three-dimensional reconstruction of the human brain: The details show the border between gray and white matter.
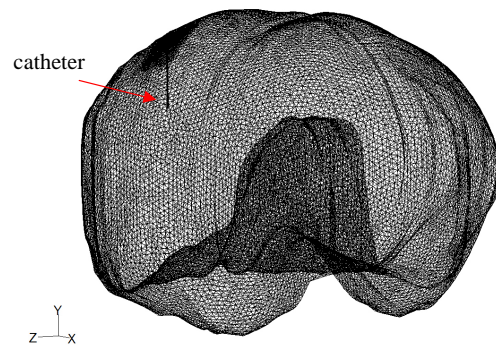

Figure 11. Three-dimensional grid of the cerebral hemispheres with a catheter.

4.2. Drug administration based on CFD techniques

The transport of a drug released from a catheter tip into the brain accounts for molecular diffusion and convective bulk flow through the porous cell matrix of the parenchyma (Reisfeld et al, 1995). The conservation equations for drug distribution are coupled with flow equations (continuity of the bulk and momentum into porous tissues for the infusate) to arrive at the governing equation of the species concentration.

$$\frac{\partial}{\partial t}(\rho C_i) + \vec{\nabla} \cdot (\rho \vec{q} C_i) = \vec{\nabla} \cdot (\rho D \vec{\nabla} C_i) + R_i \tag{5}$$

where C_i the concentration of species i in the bulk, $\vec{q}$ is the velocity vector, D is the diffusion coefficient of the drug, R_i is the rate of production of species i by chemical reaction.

$$R_i = M_i \sum_{r=1}^{N} \hat{R}_{i,r} \tag{6}$$

In equation (6), $\hat{R}_{i,r}$ is the Arrhenius molar rate of creation or destruction of the species i in reaction r, M_i is the molecular weight of species i. The reaction terms can also account for metabolic uptake of the drug. Additional sink terms may be used to model the reabsorption of the drug into the capillaries or to a permanent binding of the drug to a receptor.

The proposed model for drug infusion into the soft tissues of the human brain balances the bulk fluid (water) and the drug. The drug molecule is very dilute and is therefore not balanced in the conservation of mass equation (equation (1)). The momentum equations for interstitial fluid velocity field are described in equation (7). The equations of motion of the fluid are the Navier-Stokes equations in incompressible form (ρ = constant). In equation (7), we add an additional pressure drop that comes from the non-linear version of the Darcy's law known as the Forscheimer's law (Dullien, 1979).

$$\frac{\partial \vec{q}}{\partial t} + (\vec{q}.\vec{\nabla}\vec{q}) = -\frac{1}{\rho}\vec{\nabla}p + v\,\vec{\nabla}^2\vec{q} + S_i \tag{7}$$

The unknowns in the momentum equations are the velocity vector $\vec{q}$ as well as the pressure p. In equation (7), ρ is the infusate density and v the infusate kinematic viscosity. S_i represent the additional pressure gradient imposed by the porous tissues of the brain parenchyma (gray and white matter) to the fluid flow (infusate) and is given in equation (8).

$$S_i = -\left(\sum_{j=1}^{3} D_{ij} \mu v_j + \sum_{j=1}^{3} C_{ij} \frac{1}{2} \rho v_{mag} v_j \right) \tag{8}$$

This momentum sink contributes to the pressure gradient in the porous cell, creating a pressure drop that is proportional to the square of the fluid velocity in the cell.

4.3. Results and Discussion of Stationary Drug Delivery

The proposed methodology allows scientists to improve therapeutic approaches in a systematic fashion. Our studies aimed at increasing the penetration depth by varying the catheter location, initial concentration of drug and drug injection policy (e.g. steady, pulsating etc.). We model the brain as a porous material with different properties, like porosity, permeability and inertia resistance (see *Table 1*). The infusate – a homogenous mixture of the drug carrier and the drug molecule - is injected with the aim of establishing a convective flow field in the extracellular space. For the experiments of Figure 12 and Figure 13, the drug is injected into the right hemisphere of the three-dimensional patient specific brain geometry with a mass flow rate of $\dot{m} = 6.0 \times 10^{-8}\, kg/s$. This approach establishes a convective flow field increasing the penetration depth of the drug. Figure 12 depicts the resulting concentration of the drug in sagittal cross sections of the three-dimensional geometry from posterior to anterior. In the second sagittal cross section the injection area close to the human cortex is visible. The velocity contours shown in Figure 13 depict the convective flow field that is established due to the infusion of the chemical substance.

Table 1. Parameters used

Parameter		Value
φ – porosity	GM	0.2
	WM	0.4
k – permeability	GM	$10^{+15}\ m^{-2}$
	WM	$10^{+12}\ m^{-2}$
β – inertia resist.	GM	$10^{+4}\ m^{-1}$
	WM	$10^{+4}\ m^{-1}$
μ – viscosity		0.001
		Kg/m-s
GM : Gray Matter		
WM : White Matter		

The effect of flow field on the deformation of soft tissue with change in porosity and tortuosity cannot be neglected at very high infusion rates (P.F. Morrison et al, 1994). Our future research are directed toward solving the fully coupled fluid-structure interaction of the solid cell matrix with the infusate flow field.
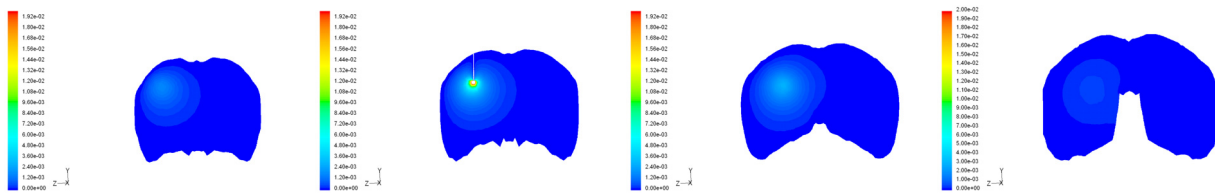

Figure 12. Concentration of the drug in sagittal sections from Posterior to Anterior (back to front).
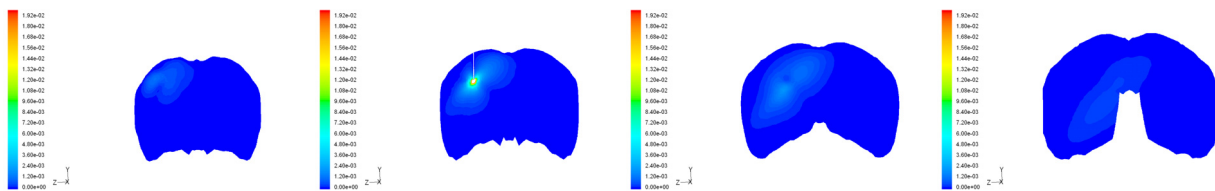

Figure 13. Velocity magnitude in sagittal sections from Posterior to Anterior (back to front).

5. Conclusions

Problem Formulation and Relevance. Novel analytical imaging techniques like MRI, functional MRI, Diffusion Tensor Imaging (DTI), Computer Tomography (CT), Positron Emission Tomography (PET), etc, improve medical diagnosis. However, the existing technologies do not directly support the use of the imaging data for devising better treatment options. There appears to be a gap between high quality of imaging techniques and the their use in quantitative analysis in the clinical practice. The sketchy understanding of the intracranial dynamics prevents the implementation of effective invasive drug delivery into the brain. In addition, more effective treatment of patients suffering from hydrocephalus cannot be expected without models for quantifying the intracranial pressure and flow of cerebrospinal fluid.

Innovation. This research proposes a novel computer-assisted brain analysis approach by integrating Mimics image reconstruction capabilities with first principles models for transport phenomena in the human brain. The therapeutic potential for this novel approach is discussed by means of two specific examples. The first one focuses on new insights pertaining to the changes in intracranial pressures (ICP) and CSF flow dynamics in hydrocephalic patients. The second example highlights new avenues for the systematic design of invasive drug delivery techniques based on patient-specific image data and molecular transport properties of neuro-pharmacological drugs.

Mimics Innovation Awards 2005: http://www.materialise.com/mimics/Awards2005_ENG.html

Social Impact. The patient specific approach will impact the medical community and the affected patients from brain disorders. This approach integrates state of-the-art imaging techniques (MRI, CT, PET and Angiogram) with the reconstruction capabilities of Mimics and first principles models for transport phenomena in order to provide better understanding of complex interactions between tissues and biological fluids in the human brain. The patient-specific approach will provide the medical community with a computer-aided tool to reduce the number of *in vivo* tests by better capitalizing on the results of fewer experiments with the help of advances computational methods. This will reduce the pain of the patient, the cost of experiments and healing procedures.

Economic Potential. The link between images and computational analysis facilitated by Mimics is expected to advance the effectiveness of scientists and engineering in assisting medical diagnosis and treatment planning. The computer-assisted brain analysis may become a standard extension of the existing patient care. The successful implementation of these novel technique might make Mimics a central element of the medical diagnostic infrastructure of hospitals treating brain diseases.

6.   References

S. Ammourah, A. Aroussi and M. Vloberghs, Cerebrospinal Fluid dynamics in a Simplified Model of the Human Ventricular System, 11th Annual Conference on CFD 2003, Vancouver BC, Canada, May 28-30, 2003.

ANSYS Inc., (Ansys), http://www.ansys.com, accessed 3/30/2005.

V. Bahl, and A.A. Linninger; Modeling of Event-Driven Continuous-Discrete Processes, Lecture Notes in Computer Science 2034, Springer Verlag, pp. 387- 402, ISBN 3-540-41866-0, 2001.

J. Bear, Y. Bachmat, *Introduction to Modeling of Transport Phenomena in Porous Media*, ed. J. Bear, **4**, Dordrecht: Kluwer Academic Publishers, 1990.

M.A. Biot, General Theory of Three-Dimensional Consolidation, Journal of Applied Physics**, 12**, pp. 155-164, 1941.

R.H. Bobo, D.W. Laske, A. Akbasak, P.F. Morrison, R.L. Dedrick, E.H. Oldfield, Convection-enchanced delivery of macromolecules in the brain, Proc. Natl. Acad. Sci. USA, **91**(3), pp. 2076-2080, 1991.

G. Bohn, P. Galuppo, A.A. Vesnaver, 3D adaptive tomography using Delaunay triangles and Voronoi polygons, Geophysical Prospecting, **48**, pp. 723-744, 2000.

CD-Adapco (Star CD) http://www.cd-adapco.com/, accessed 3/30/2005.

S. Chowdry and A.A. Linninger, Automatic Structure Analysis of Large Scale Differential Algebraic Systems, Proc. *IEEE Instrumentation and Measurement Technology Conference*, Budapest, P1-7, 2001.

F.A.L. Dullien, *Porous Media Fluid Transport and Pore Structure*, Academic Press, INC, 1979.

M. Egnor, L. Zheng, A. Rosiello, F. Gutman, R. Davis: A model of pulsations in communicating hydrocephalus. *Pediatr Neurosurg,* **36**, pp. 281-303, 2002.

D.R. Enzmann, N.J. Pelc, "Brain motion: measurement with phase-contrast MR imaging", *Radiology*, **185**(3), pp. 653-660, 1992.

C. Fletcher, *Computational Techniques for Fluid Dynamic*, Springer Verlag, 1991.

S. Hakim, J.G. Venegas, and J.D. Burton, "The physics of the cranial cavity, hydrocephalus and normal pressure hydrocephalus: mechanical interpretation and mathematical model", *Surg. Neurol.*, **5**, pp. 187-210, 1976.

J.F. Hamilton, P.F. Morrison, M.Y. Chen, J. Harvey-White, R.S. Pernaute, H. Phillips, E. Oldfield, K.S. Bankiewicz, Heparin Coinfusion during Convection-Enchanced Delivery (CED) Increases the Distribution of the Glial-Derived Neurotrophic Factor (GDNF) Ligand Family in Rat Striatum and Enhances the Pharmocological Activity of Neurturin, Experimental Neurology, **168**, pp. 155-161, 2001.

S. Kalyanasundaram, D.V. Calhoun, W.K. Leong, A finite element model for predicting the distribution of drugs delivered intracranially to the brain, American Physiological Society, pp. R1810-R1821, 1997.

E. Kandel et al., Principles of Neural Science, Appleton & Lange; 3rd edition, 1991.

S. Kondapalli and A.A. Linninger, A Model of Blood Flow through the Human Cerebral Vasculature, UIC-LPPD-110904, January 2005.

A.A. Linninger, C. Tsakiris, and R. Penn, A Systems Approach to Hydrocephalus in Humans, Seventeenth Meeting of Cybernetics and Systems Research (EMCSR 2004), Session: Systems Science in Medicine, Vienna, Austria, April 13-16, 2004.

A.A. Linninger, C. Tsakiris, D.C. Zhu, M. Xenos, P. Roycewicz, Z. Danziger, R. Penn, "Pulsatile cerebrospinal fluid dynamics in the human brain", IEEE Transactions on Biomedical Engineering, **52**(4), 2005.

Materialise, Inc., (Mimics), http://www.materialise.be/mimics/main_ENG.html, accessed 3/30/2005.

Mimics Innovation Awards 2005: http://www.materialise.com/mimics/Awards2005_ENG.html

P.F. Morrison, D.W. Laske, H. Bobo, E.H. Oldfield, L.R. Dedrick, High-flow microinfusion: tissue penetration and pharmacodynamics, American Journal of Physiology, **266**, pp. R292-R305, 1994.

T. Nagashima, B. Horwitz, S.I. Rapoport, *A mathematical model for vasogenic brain edema*, Advances in neurology **52**, pp. 317-326, 1990.

W.M. Pardridge, Non-invasive drug delivery to the human brain using endogenous blood-brain barrier transport systems, Research Focus, **2**, pp. 49-59, 1999.

S.V. Patankar, *Numerical heat transfer and fluid flow*, McGraw-Hill, New York, 1980.

R.D. Penn, M.C. Lee, A.A. Linninger, K. Miesel, S.N. Lu, L. Stylos, Pressure Gradients in the Brain: an Experimental Model in Hydrocephalus, J. Neurosurgery, 2005 (to appear).

B. Reisfeld, S. Kalyanasundaram, K. Leong, A mathematical model of polymeric controlled drug release and transport in the brain, Journal of Controlled Release, **36**, pp. 199-207, 1995.

H. Schlichting, *Boundary-Layer theory*, 7th Ed., McGraw-Hill, New York, 1979.

The Fluent, Inc, (Gambit/Fluent/FIDAP), http://fluent.com/software/, accessed 3/30/2005.

The International Center for Numerical Methods in Engineering (CIMNE - GID) http://gid.cimne.upc.es/, accessed 3/30/2005.

M. Xenos and A.A. Linninger, Large-scale fluid structure interaction modeling in the human brain, AIChE Annual Meeting, November 7-12, Austin, TX, 2004.

M. Xenos, and A.A. Linninger, Generalized Curvilinear Coordinates, UIC-LPPD-012505a, January 2005a.

M. Xenos, and A.A. Linninger, Finite Element Method, UIC-LPPD-012505b, January 2005b.

D.C. Zhu, M. Xenos, A.A. Linninger and R.D. Penn, Lateral Ventricle Motion, Cerebrospinal Fluid Movement, Visualization and Implications to the Model of Flow Dynamics, under preparation.